

Structural, microstructural, magnetic and optical behaviour of nanostructured $\text{Ni}_{0.5}\text{Zn}_{0.5}\text{Fe}_2\text{O}_4$ thin films

KANCHAN BALA*, P. SHARMA^a, N. S. NEGI

Department of Physics, Himachal Pradesh University Shimla-171005, India

^aDepartment of Physics, Jaypee University of Information Technology, Waknaghat, Solan 173215, India

$\text{Ni}_{0.5}\text{Zn}_{0.5}\text{Fe}_2\text{O}_4$ (Ni-Zn) nanocrystalline thin films were deposited on Si and quartz substrates by metallo-organic decomposition (MOD) method using spin coating technique. The films were annealed at different temperature ranging from 450^o to 700^oC for 2h. The structural properties of the samples were studied by X-ray diffraction and atomic force microscope. The influence of annealing temperature on, microstructure and magnetic properties of $\text{Ni}_{0.5}\text{Zn}_{0.5}\text{Fe}_2\text{O}_4$ thin films has been systematically investigated. The X-ray diffraction patterns confirm the formation of cubic spinel structure in these samples. The crystalline orientation of the films is changed from (311) to (400) on increasing annealing temperature to 550^oC. The crystallite size also increases from ~ 12 to 16nm. The maximum magnetization value M_s ~302 emu/cm³, was measured for Ni-Zn thin films annealed at 700^o C. The nanocrystalline thin films have shown superparamagnetic characteristic. The optical properties of $\text{Ni}_{0.5}\text{Zn}_{0.5}\text{Fe}_2\text{O}_4$ thin film annealed at 700^oC were investigated. The optical parameters such as refractive index (n), extinction coefficient (k), energy band gap, optical dielectric constant and conductivity have been extracted from the transmission spectrum measured in the wavelength range 400 -1100nm. The refractive index and extinction coefficients of the Ni-Zn film were obtained by the Swanepoel method.

(Received January 14, 2013; accepted March 13, 2014)

Keywords: Ni-Zn, nanocrystalline thin films, XRD, AFM, Magnetic and optical properties

1. Introduction

Nanocrystalline thin films of spinel ferrites are of significant interest due to their unique magnetic properties, high electrical resistivity and low eddy current losses [1-3]. Recently, the synthesis of nanocrystalline Ni-Zn ferrite thin films have received considerable attention due to their wide variety of applications in information storage, antenna rods, core transformers, sensors, medical diagnostics and ferro fluids and emulsions [4-7]. The properties of nanocrystalline thin films of spinel ferrites are strongly influenced by the cation distribution, composition and preparation technique. In bulk, ZnFe_2O_4 is a normal spinel, with Zn^{2+} ions occupy the tetrahedral sites and Fe^{3+} ions occupy the octahedral sites and it exhibits antiferromagnetic ordering below 10K. Further, Zn^{2+} is mostly incorporated at the tetrahedral lattice site, so super exchange interaction between the two sub lattices cannot be expected. Therefore, in ZnFe_2O_4 only antiferromagnetic coupling will take place [8]. In contrast, NiFe_2O_4 exhibits a mixed spinel structure with Ni^{2+} ions occupying both tetrahedral and octahedral sites that result in ferrimagnetic behavior. The magnetic properties of both NiFe_2O_4 and ZnFe_2O_4 change significantly when the grain size reduces to nanoscale. For example, Neel temperature (T_N) of ZnFe_2O_4 increases above 10K depending on particle size [9-10]. The decrease in particle size of NiFe_2O_4 promotes spin disorder on particle surface

and is considered to be a reason for ferromagnetic suppression [11-12]. The unusual and interesting properties of nanocrystalline NiFe_2O_4 and ZnFe_2O_4 have motivated us to study $\text{Ni}_{0.5}\text{Zn}_{0.5}\text{Fe}_2\text{O}_4$ mixed ferrite thin films. Ferrite nanocrystalline thin films are generally prepared by sputtering [13, 14], pulsed laser ablation [15], sol-gel [16], and spin-spraying [17] and citrate precursor method [18]. On the other hand, nanocrystalline ferrite thin films can also be easily fabricated by metallo-organic decomposition (MOD) method with distinct advantages, such as easy process ability, stable solution, low cost, controllable morphologies and crystalline sizes. In fact, synthesis in organic solvent produces a narrow crystallite size distribution [19, 20], which has tremendous advantages for magnetic nanocrystals with relaxation time that depends exponentially on volume. Even though $\text{NiZnFe}_2\text{O}_4$ nanoparticles have been studied recently, many fundamental and critical characteristics of its thin film form including structural, magnetic and optical properties still need further investigation. To our knowledge, no reports are available in the literature on magnetic and optical properties of nanocrystalline $\text{Ni}_{0.5}\text{Zn}_{0.5}\text{Fe}_2\text{O}_4$ thin films prepared by metallo-organic decomposition (MOD) method.

The aim of our work is to fabricate nanocrystalline $\text{Ni}_{0.5}\text{Zn}_{0.5}\text{Fe}_2\text{O}_4$ thin films by metallo-organic decomposition (MOD) method. We systematically

investigate the microstructure and magnetic properties of Ni_{0.5}Zn_{0.5}Fe₂O₄ thin films with varying annealing temperature. The optical properties (energy gap, refractive index and extinction coefficient) of the film annealed at 700°C are also reported.

2. Experimental details

The nanocrystalline Ni_{0.5}Zn_{0.5}Fe₂O₄ thin films were deposited by metallo-organic decomposition (MOD) technique. The films were deposited on Si and quartz substrates by sequential spin coating and bake out of the complex MOD precursor solutions followed by crystallization annealing at different temperature ranging from 450°C to 700°C for 2h. The precursor solutions were prepared using Ni(NO₃)₂·6H₂O, Zn(NO₃)₂·H₂O and Fe(NO₃)₃·9H₂O as starting materials. Nickel 2-ethylhexanoate (C₇H₁₅COO)₂Ni, Zinc 2-ethylhexanoate (C₇H₁₅COO)₂Zn, and Iron 3-ethylhexanoate (C₇H₁₅COO)₃Fe precursors were synthesized from these starting materials. The details of precursor synthesis are given elsewhere [21]. The coating solution was prepared by mixing the precursors in the require molar ratio of Ni : Zn : Fe :: 0.5 : 0.5 : 2 in xylene. Xylene and polyethylene glycol were used as the solvent and polymerizing agents, respectively. MOD precursor solution was spin coated at 4500 rpm for 60s followed by bake out at 350°C for 5 min to remove the organic residuals and to induce reaction between constituents. The spin-on coating and drying steps were sequentially repeated for four times to build-up a film thickness. A post-deposition isothermal annealing of spin-on coating at 450°, 550°, 650° and 700°C for 2h leads to crystallization of the Ni_{0.5}Zn_{0.5}Fe₂O₄ thin films. The crystalline structure of Ni_{0.5}Zn_{0.5}Fe₂O₄ thin films was examined by X-ray diffraction (X-Pert PRO). Film morphology and surface roughness were investigated by atomic force microscopy (VECCO DI CP-II) in the contact mode. Magnetic measurements of the films were performed at room temperature by a vibrating sample magnetometer (VSM, Microsense, USA) with a magnetic field up to 20 kOe. The optical transmittance of the thin films was measured using a Parkin Elmer UV-0637 spectrophotometer in the wavelength range from 400 to 1100nm.

3. Result and discussion

Fig. 1, shows the X-Ray diffraction (XRD) patterns of Ni_{0.5}Zn_{0.5}Fe₂O₄ thin films annealed at temperature range 450°–700°C for 2h. The XRD results show that Ni-Zn films have cubic spinel structure with peak intensity increases with increase in the annealing temperature. The

reflection lines (220), (311), (400), (422) and (511) are observed at diffraction angle 2θ = 30.18, 35.45, 43.51, 50.92 and 57.17 respectively for the film annealed at 450°C, which are well matched with reflections of Ni_{0.5}Zn_{0.5}Fe₂O₄ ferrite reported in the standard card (JCPDS card # 052-0278). The XRD pattern shows a change in most intense peak from (311) to (400) as the annealing temperature increases. The minor impurity peaks corresponding to Fe₃O₄ are completely eliminated on increasing the annealing temperature to 700°C. It is also observed that the diffraction peaks become narrower and sharper with the augment of heat treatment temperature indicating the increase in crystallite size, which is consistent with the values of crystallite size as calculated by using Scherrer equation at (400) peaks:

$$D = \frac{0.9\lambda}{\beta \cos \theta} \quad (1)$$

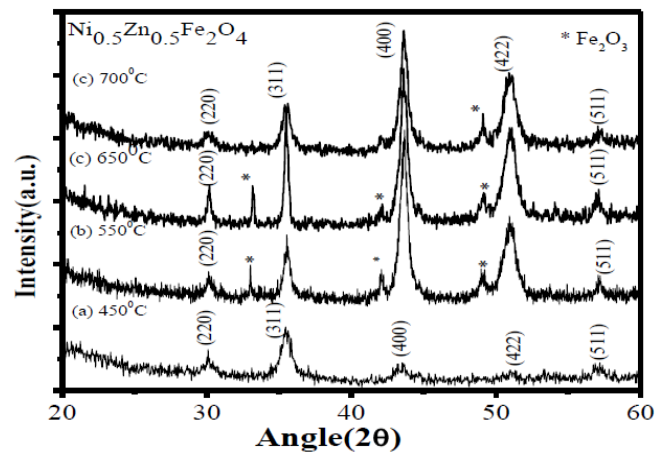


Fig. 1. XRD patterns of Ni_{0.5}Zn_{0.5}Fe₂O₄ thin films annealed at (a) 450°C, (b) 550°C, (c) 650°C and (d) 700°C.

Where D is the crystallite size, λ is the wavelength of Cu-K α , β is the full width at half maximum (FWHM) of the diffraction peaks, and θ is the Bragg angle. The lattice constant 'a' for cubic crystal system was calculated using the equation

$$a = d\sqrt{h^2 + k^2 + l^2} \quad (2)$$

Where hkl are the miller indices of the diffraction peak and d is the interplanar spacing. From Fig. 2 it indicates that the grain size increases from ~ 12 to 16nm due to grain growth in thin film as the annealing temperature increases. The lattice constant decreases from 8.328 to 8.291Å with increase in annealing temperature from 450°C to 700°C. Increase in grain size is expected with the increase in

annealing temperature because of increase in the surface mobility of atoms, which allows the film to decrease its total energy by growing larger grains and decreasing their grain boundary area [22]. The decrease in lattice constant may be attributed to densification of the film with increasing annealing temperature. The decrease in lattice constant of nanocrystalline Ni-Zn thin films could also be explained on the basis of the cation distribution with annealing temperature. In other words, Zn^{2+} ion (ionic radius 0.74 Å) has a small amount of evaporation loss with increasing annealing temperature, and this will cause part of Ni^{2+} (ionic radius 0.69 Å) substituting the Zn^{2+} site, which leads to the decrease of the lattice constant as evidenced by the (400) peak shift to a higher 2θ position. Figs. 3(a) to (d) show amplitude images of AFM micrographs of Ni-Zn thin films annealed at temperatures 450°, 550°, 650° and 700°C respectively. Figs. 3(e) to (h) represent their respective angular view images. The pictures reveal highly dense and smooth films with well nanocrystallinity constructed by round grains with narrow size distribution, typically ranging between 3.6 and 8.8nm corresponding to the annealing temperatures 450°C to 700°C. The results are in good agreement with the XRD observations. Furthermore, values of root mean square roughness are measured in the range of 0.3 to 1.5nm, which demonstrates that the deposited films are fairly flat. Figs. 4(a) shows typical results for magnetization curves of Ni-Zn thin films annealed at different temperatures. The dependence of the magnetic properties of Ni-Zn thin films on annealing temperature is evident. It is seen that the maximum applied field of 20kOe is not enough to saturate the films annealed at temperature 650° and 700°C. The maximal magnetization values measured at room temperature are 116, 245, 297 and 302 emu/cm³ respectively, for films annealed at temperatures 450°, 550°, 650° and 700°C. The high values of the magnetization for $Ni_{0.5}Zn_{0.5}Fe_2O_4$ thin films are due to the higher value of magnetic moments by considering the mixed cationic distribution. In the inverse spinel structure magnetic moments of Ni^{2+} ($3\mu_B$) ions play a crucial role in controlling the magnetic properties because Fe^{3+} ($5\mu_B$) ions cancel each other at their respective sites [23]. The higher value of magnetic moment compared with the inverse spinel for mixed cationic distribution is expected

due to the presence of Ni^{2+} at tetrahedral site. It can be seen in Fig. 4(a) that magnetization increases with increasing the annealing temperature from 450°C to 700°C. The enhancement in magnetization with increasing annealing temperature is attributed to the increase in grain size. The average grain size calculated by using Scherrer formula from XRD peak as well as measured from AFM images were found to increase as the annealing temperature increased from 450° to 700°C. The increase of magnetization with the grain size in nanocrystalline ferrite films is generally observed and is well established phenomenon [24]. The magnetizing mechanism in ferrites arises from spin domain rotation and domain wall motion. The domain wall motion is influenced by grain size and annealing parameter and is enhanced by increase in grain size [25-26]. In smaller grain size, increase in surface to volume ratio promotes random spin canting on the crystal surface [27]. This causes a decrease in magnetization with decreasing grain size. In Fig. 4(b) there is no hysteresis for the magnetization curves measured for $Ni_{0.5}Zn_{0.5}Fe_2O_4$ thin films i.e. both the retentivity and coercivity are zero. The result indicates that the nanocrystalline $Ni_{0.5}Zn_{0.5}Fe_2O_4$ thin films behave superparamagnetically at the annealing temperature ranging from 450° to 700°C.

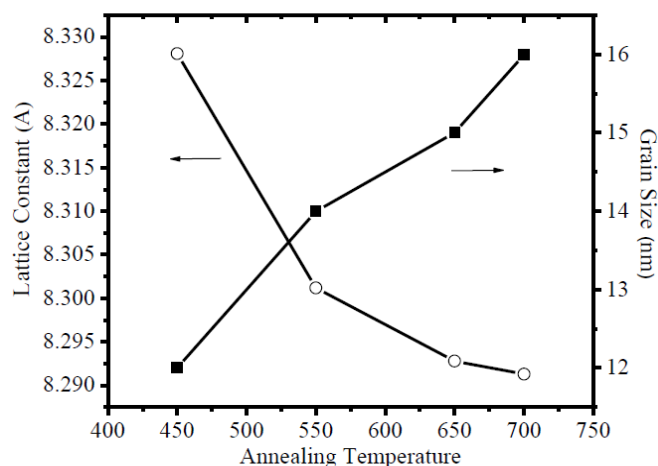


Fig. 2. Variation of lattice parameter and grain size of $Ni_{0.5}Zn_{0.5}Fe_2O_4$ thin films with annealing temperature.

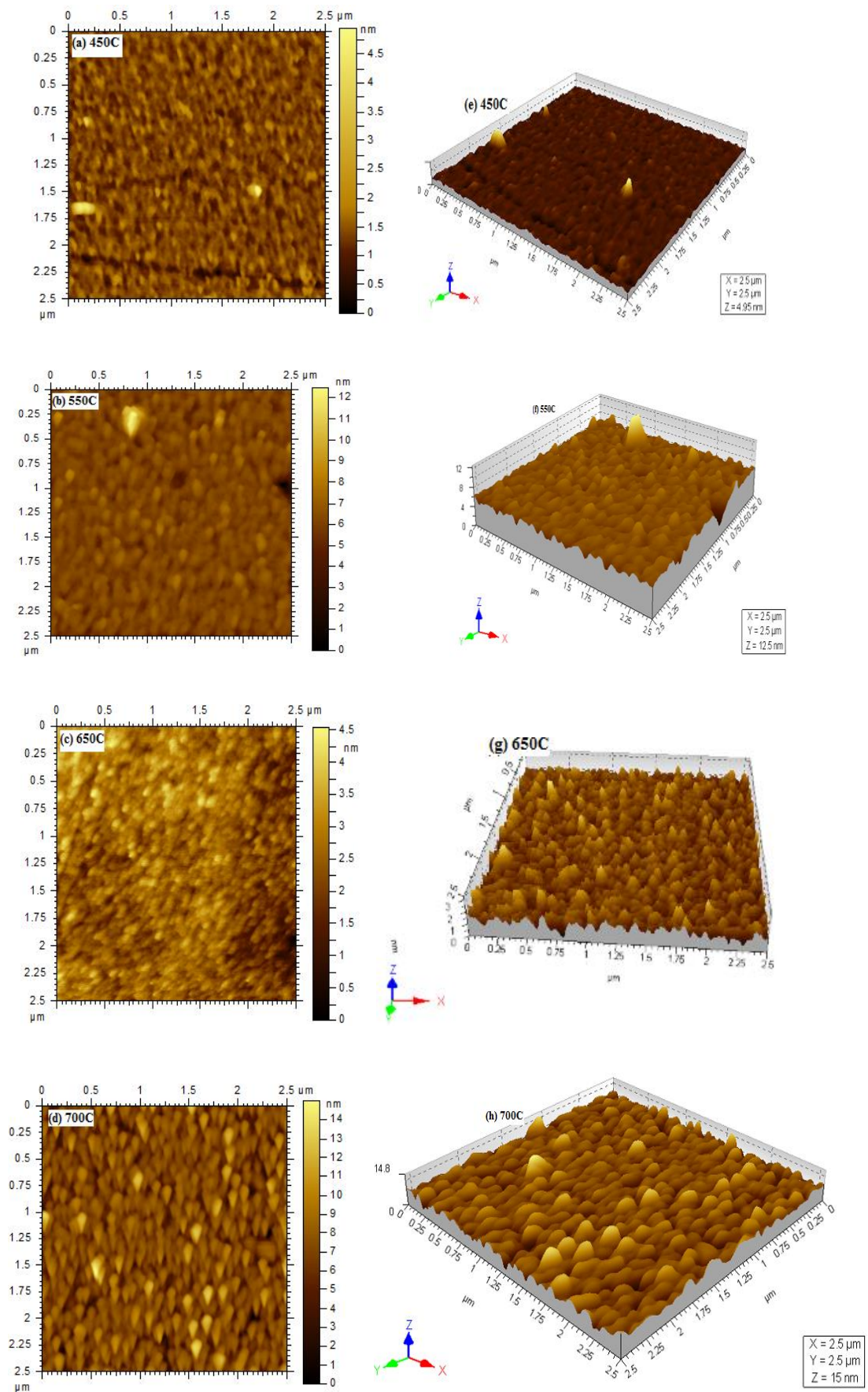


Fig. 3. AFM images of $\text{Ni}_{0.5}\text{Zn}_{0.5}\text{Fe}_2\text{O}_4$ thin films (a) to (d) Amplitude images and (e) to (f) Angular view.

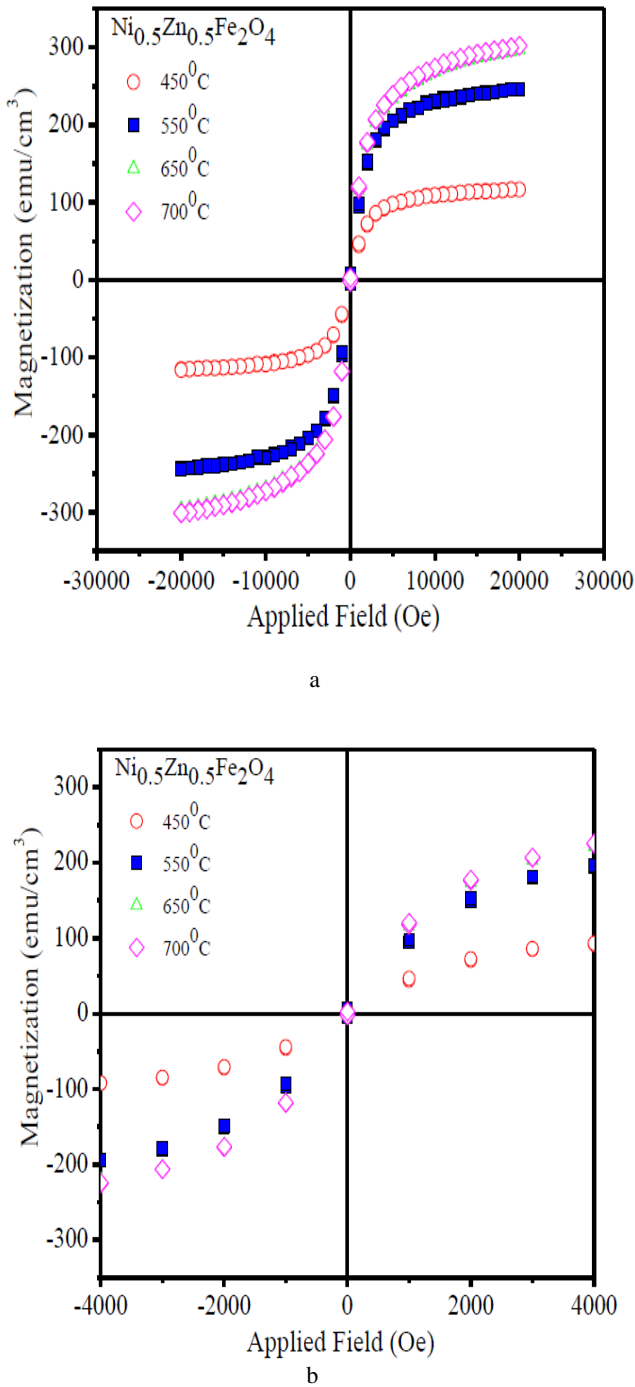


Fig. 4. Room temperature magnetic properties of $Ni_{0.5}Zn_{0.5}Fe_2O_4$ thin film films deposited on Si substrates (a) M-H curves and (b) smaller scale view.

The optical properties of the $Ni_{0.5}Zn_{0.5}Fe_2O_4$ thin film on quartz substrate have been determined using the fringe pattern method. Transmission (T) versus wavelength (λ) curve of $Ni_{0.5}Zn_{0.5}Fe_2O_4$ (Ni-Zn) thin film annealed at $700^\circ C$ is shown in Fig. 5. The film shows high transmittance $> 80\%$. According to Swanepoel [28] the value of the refractive index of the film can be calculated by using the following expression. In the transparent

region, where the absorption coefficient $\alpha \approx 0$, the refractive index (n) is given by

$$n = [N + (N^2 - S^2)^{1/2}]^{1/2} \quad (3)$$

Where

$$N = \frac{2S}{T_m} - \frac{(S^2 + 1)}{2} \quad (4)$$

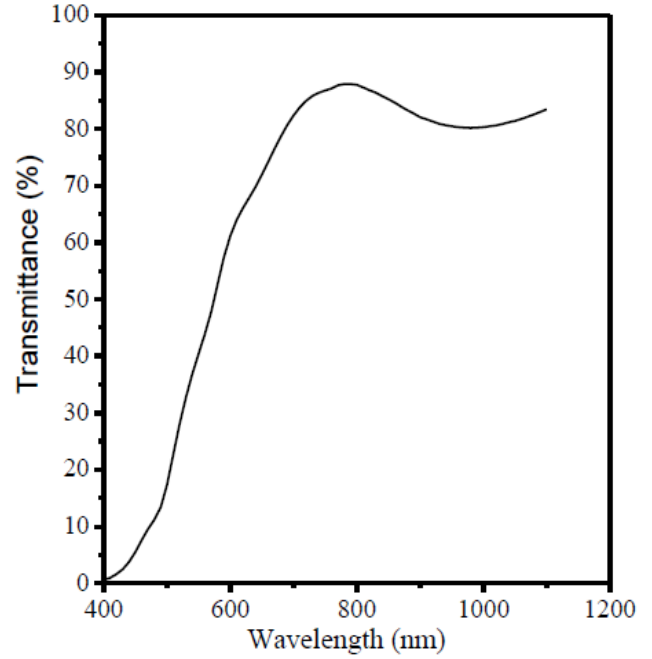


Fig. 5. Transmission versus wavelength for $Ni_{0.5}Zn_{0.5}Fe_2O_4$ thin film films deposited on quartz substrates and annealed at $700^\circ C$ for 2hr.

T_m is the envelope function of minimum transmittance and S is the refractive index (for quartz substrate, $S=1.46$) of the substrate. In the weak region where α is not equal to zero the transmittance decreases due to the influence of α and equation (4) becomes

$$N = 2S \frac{T_M - T_m}{T_M T_m} + \frac{(S^2 + 1)}{2} \quad (5)$$

Where, T_M and T_m are the transmission values corresponding to the tangent points between the upper and lower envelopes, respectively. The film thickness, d , was obtained using the relationship

$$d = \frac{\lambda_1 \lambda_2}{2(\lambda_1 n_2 - \lambda_2 n_1)} \quad (6)$$

Where, n_1 and n_2 are the refractive indices of two adjacent maxima or minima at wavelengths λ_1 and λ_2 , respectively. The calculated values of d for Ni-Zn thin film is 525nm.

The extinction coefficient (k) can be calculated using the relation

$$k = \frac{\alpha\lambda}{4\pi} \quad (7)$$

Where, α is the absorption coefficient and is given by

$$\alpha = \left(\frac{1}{d}\right) \ln\left(\frac{1}{x}\right) \quad (8)$$

Where, x is the absorbance.

In the region of weak and medium absorption using the transmission maxima, x can be calculated by

$$x = \frac{E_M - [E_M^2 - (n^2 - 1)^3(n^2 - s^4)]^{1/2}}{(n-1)^3(n-s^2)} \quad (9)$$

Where,

$$E_M = \frac{8n^2S}{T_M} + (n^2 - 1)(n^2 - S^2) \quad (10)$$

Fig. 6 shows the variation of refractive index (n) and extinction coefficient (k) with the wavelength for nanocrystalline Ni-Zn thin films annealed at 700°C. The calculated values of the refractive index of the Ni-Zn thin film is high and the transmission spectra extended up to the lower visible region. Thus nanocrystalline Ni-Zn films absorb more light, which makes highly confined waveguides and results in dense optical signals. The observed value of extinction coefficient (k) indicates low loss of light during scattering and absorption. The dispersion of the refractive index has been analyzed by using the Wemple-DiDomenico model [29], which is based on the single oscillator formula

$$n^2 - 1 = \frac{E_d E_o}{E_o^2 - (h\nu)^2} \quad (11)$$

Where, $h\nu$ is the photon energy, n is the refractive index, E_o is the single oscillator energy, also called the average energy gap, and E_d is the dispersion energy, which is a measure of the average strength of the interband optical transitions. Moreover, it can be seen that experimental variation in the refractive index deviates from that given by equation (11), when the photon energy attains the optical gap value [30]. The oscillator energy is 'an average' energy gap, and to a very good approximation it matches with the optical-band gap E_g^{opt} . Also, $E_o \approx 2 \times E_g^{\text{opt}}$ from where values of E_g^{opt} can be determined and is given in Table 1. The real and imaginary parts of optical dielectric constant are shown in Fig. 7 by the relations [31]

$$\varepsilon_r = n^2 - k^2 \quad (12)$$

And

$$\varepsilon_i = 2nk \quad (13)$$

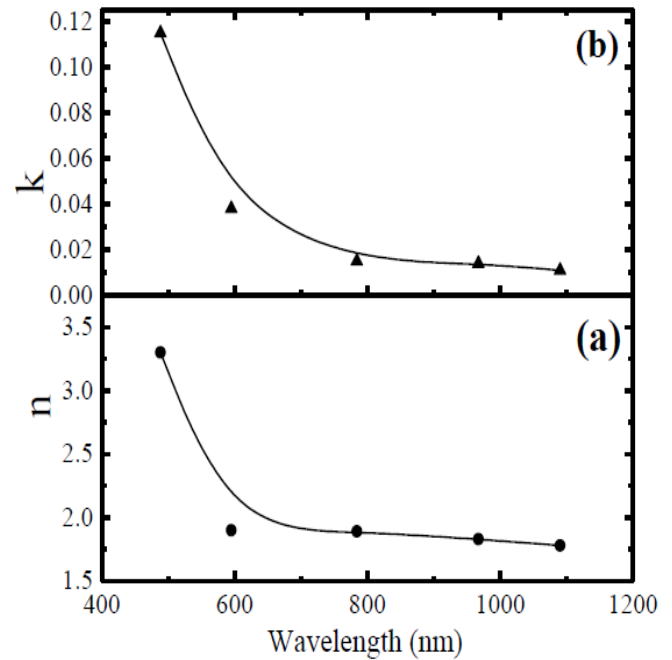


Fig. 6. Variation of refractive index (n) and extinction coefficient (k) with wavelength.

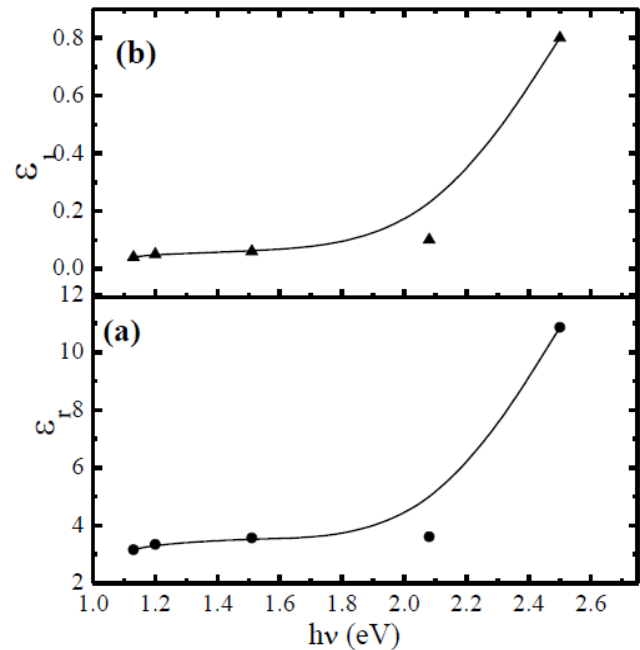


Fig. 7. Variation of optical dielectric constant (ε_r) and loss factor (ε_i) with photon energy ($h\nu$).

Table 1. Values of grain size (x), optical film thickness (d), static refractive index (n_0), single oscillator energy (E_0), dispersion energy (E_d) and optical energy band gap (E_g^{opt}) for $Ni_{0.5}Zn_{0.5}Fe_2O_4$ thin film annealed at $700^\circ C$.

Annealing Temperature	X (crystallite size) nm	d (Thickness) nm	n_0	E_0 (eV)	E_d (eV)	E_g^{opt} (eV)
$700^\circ C$	16	525	1.70	2.99 ± 0.02	5.54 ± 0.5	1.49 ± 0.01

Fig. 8 shows optical conductivity versus photon energy for $Ni_{0.5}Zn_{0.5}Fe_2O_4$ thin film and is given by the relation [32]. The real part of the dielectric constant indicates the speed of light when it is transmitting through nano grains, and the imaginary part shows how a dielectric absorbs energy from an electric field due to dipole motion. The value of dielectric constant is 3.6 observed at higher energy of 2.08 eV for Ni-Zn thin film annealed at $700^\circ C$. The optical conductivity means how the dielectric can absorb light during scattering process. This absorption of light is given by plotting the optical conductivity

$$\sigma = \frac{\alpha n c}{4\pi} \quad (14)$$

Where, c is the velocity of light, α is the absorption coefficient and n is the refractive index. The optical conductivity is found to increase sharply after 1.51 eV. At this energy region, the observed values of optical conductivity are in the range of $10^{11} s^{-1}$. From MH hysteresis curve and small grain size, we can conclude that $Ni_{0.5}Zn_{0.5}Fe_2O_4$ thin films have super paramagnetic behavior. Therefore due to super paramagnetic behavior

and high transmittance, it may have magneto-optical applications in the visible spectral range.

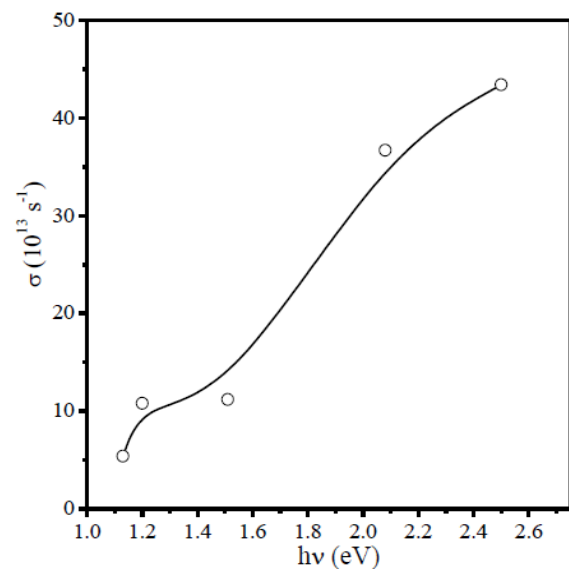


Fig. 8. Optical conductivity (σ) versus photon energy ($h\nu$).

Table 2. Values of Crystallite size (XRD), grain size (AFM), magnetization and Bohr magneton for $Ni_{0.5}Zn_{0.5}Fe_2O_4$ thin film annealed at $450^\circ C$, $550^\circ C$, $650^\circ C$, $700^\circ C$.

Annealing Temperature	Crystallite size (XRD)	Grain size (AFM)	Magnetization (emu/cc)	Bohr magneton (μ_B)
$450^\circ C$	12nm	5nm	116emu/cc	1.37
$550^\circ C$	13.5nm	12nm	245emu/cc	2.91
$650^\circ C$	15nm	12.5nm	297emu/cc	3.41
$750^\circ C$	16nm	15nm	302emu/cc	3.51

4. Conclusion

In this study, $Ni_{0.5}Zn_{0.5}Fe_2O_4$ (Ni-Zn) nanocrystalline thin films have been fabricated on Si and quartz substrates by metallo-organic decomposition (MOD) method. The structural, morphological, magnetic and optical properties of Ni-Zn thin films were investigated as a function of annealing temperature. The XRD pattern revealed that the cubic spinel structure is maintained for all the nanocrystalline films annealed at temperature range 450 to

$700^\circ C$. The study shows that the most intense peak of the film changes from (311) to (400) on increasing annealing temperature to 550, 650 and $700^\circ C$. The lattice constant of Ni-Zn thin film increases from 8.328 to 8.291 Å with increase in annealing temperature from $450^\circ C$ to $700^\circ C$. The grain size increases from 5 to 10nm. Overall microstructures of all $Ni_{0.5}Zn_{0.5}Fe_2O_4$ thin films as revealed from AFM images show dense, homogeneous, smooth micrograph. With the increase of annealing temperature, the magnetization value M_s enhances from 116 to 302

emu/cm³. The films exhibit superparamagnetic behavior at all annealing temperatures. The optical properties of Ni_{0.5}Zn_{0.5}Fe₂O₄ thin film such as refractive index (n), extinction coefficient (k), energy band gap, optical dielectric constant and conductivity have been calculated from the transmission spectrum of film annealed at 700°C.

Acknowledgement

We are thankful to the Department of Physics, Himachal Pradesh University, Shimla for providing the research facilities. We also thank Prof. Ravi Kumar of the National Institute of Technology Hamirpur for his help in the atomic force microscopy.

References

- [1] S. Son, M. Taheri, E. Carpenter, V. G. Harris, M. E. McHenry, *J. Appl. Phys.* **91**, 7589 (2002)
- [2] Alex Goldman, *Modern Ferrite Technology*, 2nd ed. Springer, New York, (2006).
- [3] N. Ponpandian, P. Balaya, A. Narayanasamy. *J. Phys. Condens. Matter* **14**, 3221 (2002).
- [4] M. A. Ahmed, S. T. Bishay, *J. Magn. Magn. Mater.* **279**, 178 (2004).
- [5] D. Souriou, J. L. Mattei, A. Chevalier, P. Queffelec, *J. Appl. Phys.* **107**, 09A518 (2010).
- [6] J. Philip, G. Gnanaprakash, T. Jayakumar, P. Kalyanasundaram, B. Raj, *Phys. Rev. Lett.* **89**, 268301 (2002).
- [7] J. Philip, G. Gnanaprakash, T. Jayakumar, P. Kalyanasundaram, O. Mondain-Monval, B. Raj, *Langmuir* **18**, 4625 (2002).
- [8] G. A. Petitt, D. W. Forester, *Phys. Rev. B* **4**, 3912 (1971).
- [9] J. H. Shim, S. Lee, J. H. Park, S. J. Han, Y. H. Jeong, Y. W. Cho, *Phys. Rev. B* **73**, 064404 (2006).
- [10] S. J. Stewart, S. J. A. Figueroa, J. M. Ramallo Lopez, S. G. Marchetti, J. F. Bengoa, R. J. Prado, F. G. Requejo, *Phys. Rev. B* **75**, 073408 (2007).
- [11] M. Sertkol, Y. Koeogu, A. Baykal, H. Kavas, A. C. Basaran, *J. Magn. Magn. Mater.* **321**, 157 (2009).
- [12] A. C. F. M. Costa, E. Tortella, M. R. Morelli, R. H. G. A. Kiminami, *J. Magn. Magn. Mater.* **256**, 174 (2003).
- [13] M. Sultan, R. Singh, *J. Phys. D: Appl. Phys.* **42**, 115306 (2009).
- [14] Y. Cheng, H. Liu, H. B. Li, R. K. Zheng, S. P. Ringer, *J. Phys. D: Appl. Phys.* **42**, 215004 (2009).
- [15] M. Bohra, S. Prasad, N. Kumar, D. S. Misra, S. C. Sahoo, N. Venkataramani, R. Krishnan **67**, 98 (2006).
- [16] P. Gao, E. V. Rebrov, T. M. W. G. M. Verhoeven, J. C. Schouten, R. Kleismit, G. Koziowski, J. Cetnar, Z. Turgut, G. Subramanyam, *J. Appl. Phys.* **107**, 044317 (2010).
- [17] G. Caruntu, I. Dumitru, G. G. Bush, D. Caruntu, C. J. O. Connor, *J. Phys. D: Appl. Phys.* **38**, 811 (2005).
- [18] N. Gupta, A. Verma, S. C. Kashyap, D. C. Dube, *J. Magn. Magn. Mater.* **308**, 137 (2007).
- [19] V. F. Puentes, K. M. Krishnan, A. P. Alivisatos, *Science*, **291**, 2115 (2001).
- [20] Y. Bao, K. M. Krishnan, *J. Magn. Magn. Mater.* **293**, 15 (2005).
- [21] A. Sharma, K. Parmar, R. K. Kotnala, N. S. Negi, *Int. J. Advan. Engg. & Tech.* **5**, 544 (2012).
- [22] M. W. Cole, C. Hubbard, E. Ngo, M. Ervin, M. Wood, R. G. Geyer: *J. Appl. Phys.* **92**, 475 (2002).
- [23] J. Jacob, K. M. Abdul, *J. Appl. Phys.* **107**, 114310 (2010).
- [24] M. Desai, J. Dash, I. Samajdar, N. Venkataramani, S. Prasad, P. Krishan, N. Kumar, *J. Magn. Magn. Mater.* **231**, 108 (2001).
- [25] C. Caizer, *J. Magn. Magn. Mater.* **251**, 304 (2002).
- [26] H. Zhang, Z. Ma, J. Zhou, Z. Yue, L. Li, Z. Gui, *J. Magn. Magn. Mater.* **213**, 304 (2000).
- [27] C. Caizer, *Mater. Sci. Eng. B* **100**, 63 (2003).
- [28] R. Swanepoel, *J. Phys. E: Sci. Instrum. E* **16**, 1214 (1983).
- [29] S. H. Wemple, *Phys. Rev. B* **7**, 3767 (1973).
- [30] I. Solomon, M. P. Schmidt, C. Senemaud, M. K. Driss, *Phys. Rev. B* **38**, 13263 (1988).
- [31] Q. Ren, Y. T. Chow, F. Q. Meng, S. W. Wang, Z. H. Lu, C. B. Ma, H. Wang, D. Xu, W. A. Gambling, *J. Mater. Sci.* **36**, 1857 (2001).
- [32] J. I. Pankov, *Optical Process in Semiconductors* Dover. New York, (1975).

*Corresponding author: bala.kanchan1987@gmail.com